Math Geosci (2018) 50:569–584
https://doi.org/10.1007/s11004-017-9719-5

SPECIAL ISSUE

Accurate Ocean Bottom Seismometer Positioning Method Inspired by Multilateration Technique

Omar Benazzouz[1] · Luis M. Pinheiro[1] · Luis M. A. Matias[2] · Alexandra Afilhado[3] · Daniel Herold[4] · Seth S. Haines[5]

Received: 15 April 2016 / Accepted: 14 November 2017 / Published online: 8 January 2018

Abstract The positioning of ocean bottom seismometers (OBS) is a key step in the processing flow of OBS data, especially in the case of self popup types of OBS instruments. The use of first arrivals from airgun shots, rather than relying on the acoustic transponders mounted in the OBS, is becoming a trend and generally leads to more accurate positioning due to the statistics from a large number of shots. In this paper, a linearization of the OBS positioning problem via the multilateration technique is discussed. The discussed linear solution solves jointly for the average water layer velocity and the OBS position using only shot locations and first arrival times as input data.

Keywords OBS positioning · Multilateration · Linearization

1 Introduction

Determining the true seafloor position of ocean bottom seismometers (OBS) is a subject of utmost importance. This is especially true when using the free fall method for OBS deployment, where nodes are dropped from the deck of the ship at a sea-surface location and slowly fall to the seafloor. The positioning issue causes problems

✉ Omar Benazzouz
gibnem@gmail.com

1 Department of Geosciences, University of Aveiro, Aveiro, Portugal

2 Instituto Dom Luiz, Faculdade de Ciências, Universidade de Lisboa, Lisbon, Portugal

3 Instituto Superior de Engenharia de Lisboa, Instituto Politecnico de Lisboa, Lisbon, Portugal

4 Parallel Geoscience Corporation, Crystal Bay, NV, USA

5 Central Energy Resources Science Center, United States Geological Survey, Denver, CO, USA

during the entire OBS data processing sequence (Oshida et al. 2008; Ao et al. 2010; Imtiaz et al. 2013). One procedure for the positioning of each instrument is as follows: (i) deploy the OBS at the desired sea-surface position and wait for it to reach the seafloor, (ii) steam around the instrument deployment location in circles with a radius usually up to half the water depth and spanning a range of azimuths, and (iii) determine the location of that specific OBS using an acoustic range measurement system mounted on the OBS (Shiobara et al. 1997; Oshida et al. 2008; Haines et al. 2014). This method is very time-intensive; the slowest parts of the process are the OBS free fall and the acoustic shooting time, but, as discussed in a U.S. Geological Survey report (Haines et al. 2014), quality control of data points may sometimes add a significant amount of time and can be expensive as well.

To address these issues, several authors have proposed inversion schemes using airgun first arrivals energy and sometimes using additional supportive data to determine more accurately and consistently the OBS position. Oshida et al. (2008) proposed a non-linear inversion of the first arrival times jointly with a precise bathymetric grid of the study area. Ao et al. (2010) discussed a method based on forward ray tracing and curve fitting of first arrival times and compared it to his Monte-Carlo-based curve fitting method. Imtiaz et al. (2013) proposed another approach, inverting for OBS positions and average water layer velocity for all shot lines and nodes simultaneously using an iterative least-squares method. The core of all the above-mentioned methods is a non-linear inversion, which makes sense as the unknown OBS position is non-linearly related to the measured time of the first arrivals. A linear solution to the problem was developed using a multilateration-like technique in Benazzouz et al. (2015); in this paper the OBS position and the average water layer velocity were solved simultaneously.

Multilateration is a method that is very well known in surveillance and air traffic control operations (Mantilla Gaviria et al. 2013). It is based on the measurement of the difference in distance, or arrival times, to multiple stations at known locations that broadcast signals at known times. Data from two stations result in an infinite number of locations that satisfy the measurement, representing, essentially, a hyperbolic curve in the two-dimensional case and one half of a two-sheeted hyperboloid in the three-dimensional case. A second pair of stations produces a second hyperbola that intersects the first one, and the two curves together minimize the number of possible locations to those around the intersection area. Multilateration relies on the differential measurements of multiple stations to converge from possible locations toward the exact location. In order for the multilateration technique to work properly, the stations used for measurements have to be placed at strategic locations to avoid an ill-conditioned system of equations; this is typically known as a sensor placement problem for target localization. In case one can control $x/y/z$ of each station, the location of each station can be optimized to improve the accuracy of the solution (Mantilla Gaviria et al. 2013; Domingo-Perez et al. 2016).

Benazzouz et al. (2015) presented a multilateration technique to solve jointly for the OBS position and the water layer average velocity. The work presented in the 2015 paper was only tested on synthetic data and a small two-dimensional field dataset. In this paper, the method will be further discussed and tested on a much larger field OBS dataset with three-dimensional source and receiver geometry. A general error analysis

of the method will then be presented, followed by an analysis of positioning errors introduced by each factor separately (i.e., errors in arrival times picks, low azimuthal coverage, and other factors).

2 The Control Datasets: Green Canyon—Gulf of Mexico

The Green Canyon dataset was acquired by the U.S. Geological Survey in the Gulf of Mexico in 2013 to refine geophysical methods for gas hydrate characterization and achieve improved imaging of established gas hydrate study sites, as described by Haines et al. (2014). The acquisition was conducted onboard the *R/V Pelican* and used two 105 $in.^3$ airguns as seismic sources. In the Green Canyon 955 protraction area (GC955), 21 OBS were deployed and almost 400 km of high-resolution seismic data were shot in a grid with line spacing as small as 50 m and along radial lines that provide broad azimuthal coverage, as well as source offsets of up to 10 km for the OBS. For OBS deployment, they were dropped by free fall from the sea surface in carefully selected locations. The water depth in this location is around 2000 m, and the sink time for each OBS was around 30 min. The lateral drift was anticipated to be potentially as large as a few hundred meters. Figure 1 shows the study area and a portion of the acquisition grid.

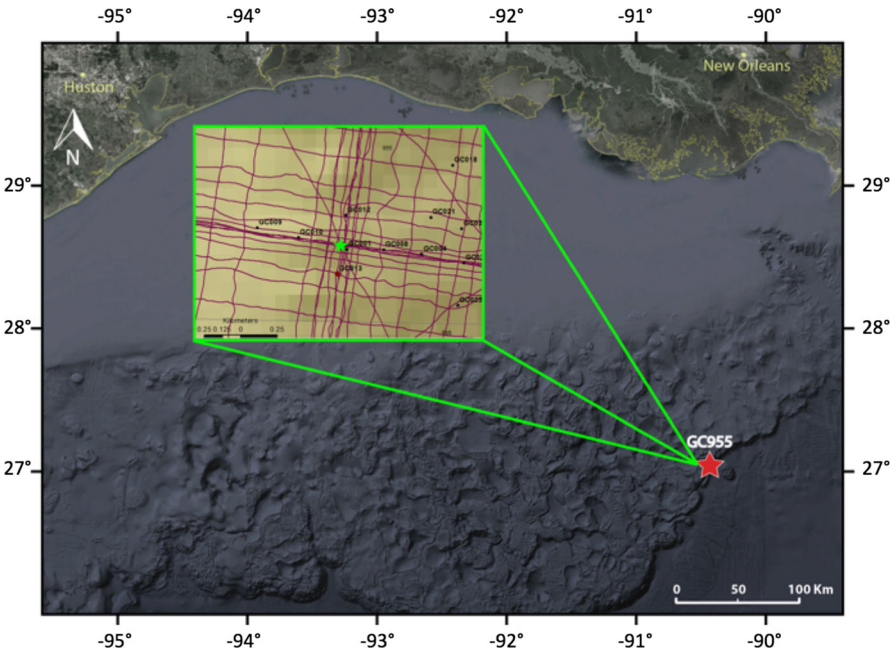

Fig. 1 Map showing the Gulf of Mexico and the Green Canyon 955 study area (red star). The green box shows a portion of the acquisition grid and the green star shows the location of the OBS used throughout this paper. Red lines indicate seismic transects, and black dots indicate OBS positions

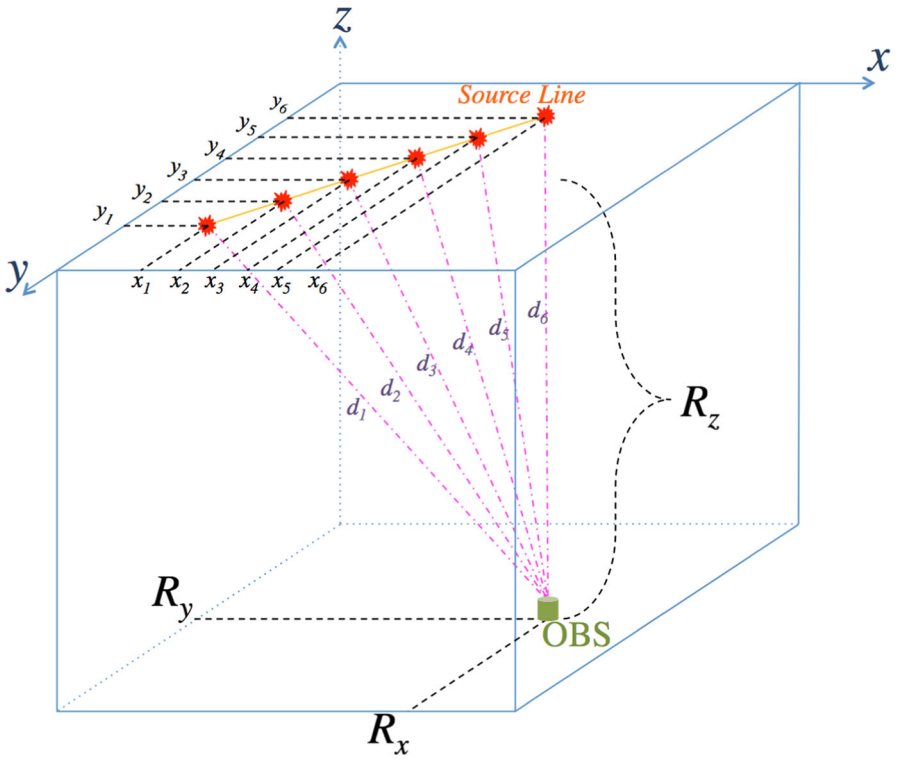

Fig. 2 OBS acquisition sketch with sources and receiver (OBS) coordinates, d_1 to d_6 are the distances between each source and the OBS

3 Method

Figure 2 shows a sketch of the OBS acquisition scenario. Here, a single source line is used for simplicity. The position of each source is known and the distance between each source and the OBS is known only in terms of time of direct arrivals, but the water layer velocity remains unknown. The considerations in this section apply to all of the following equations. All coordinates are given in a Cartesian coordinate system x, y, z (with z taken as positive downward); in fact, this is the case when using the universal transverse mercator (UTM) coordinate system, which uses a two-dimensional Cartesian coordinate system.

Let S_i (with $i = 1{-}6$ in this case, and from 0 to n in real life scenario) represent sources with coordinates x_i, y_i, and z_i, and let t_i and d_i represent, respectively, the time and distance between the source S_i and the OBS. The OBS coordinates are R_x, R_y, and R_z. This problem can be understood as finding the intersection point of multiple pseudo-spheres (the shape of the corresponding wavefronts), the center of each is at a source location S_i (x_i, y_i, z_i) with a radius equal to the distance d_i corresponding to each source-receiver pair.

Assumption The sound speed in the water layer is not constant, but can reasonably be averaged along a vertical or pseudo-vertical path. Under this assumption, the distance between each source and the receiver is simply given by

$$d_i = v_{\text{avg}} t_i \quad i = 0, 1, \ldots, n. \tag{1}$$

Consequences of this assumption will be addressed in Sect. 4 of this document.

The distance between each source and the OBS (d_i) can then be expressed in terms of arrival time and an average unknown water layer velocity

$$d_i{}^2 = v_{\text{avg}}^2 t_i^2 = (x_i - R_x)^2 + \left(y_i - R_y\right)^2 + (z_i - R_z)^2. \tag{2}$$

Here, the unknown OBS position is non-linearly related to the measured arrival time t_i and source positions. In order to linearize the problem and solve simultaneously for the OBS position and the average water layer velocity, a straightforward multilateration scheme will first be used. The distance between a given shot location (S_0 for simplicity) and the unknown OBS position (d_0) will be subtracted from other such distances (d_i with $i = 1, 2, \ldots, n$). By doing this, a new set of linear equations are obtained, each in the following form

$$\begin{aligned} d_i{}^2 - d_0{}^2 = &\left\{x_i{}^2 - 2R_x x_i + R_x{}^2 + y_i{}^2 - 2R_y y_i + R_y{}^2 + z_i{}^2 - 2R_z z_i + R_z{}^2\right\} \\ &- \left\{x_0{}^2 - 2R_x x_0 + R_x{}^2 + y_0{}^2 - 2R_y y_0 + R_y{}^2 + z_0{}^2 - 2R_z z_0 + R_z{}^2\right\}. \end{aligned} \tag{3}$$

Simplifying Eq. (3) and replacing d_i as in Eq. (2) gives

$$\begin{aligned} &R_x\,(x_0 - x_i) + R_y\,(y_0 - y_i) + R_z\,(z_0 - z_i) + v_{\text{avg}}^2\left(t_0{}^2 - t_i{}^2\right)/2 \\ &\quad = \left(x_0{}^2 - x_i{}^2 + y_0{}^2 - y_i{}^2 + z_0{}^2 - z_i{}^2\right)/2. \end{aligned} \tag{4}$$

Giving a large number of sources (more than 5), this will represent an over determined set of linear equations on four unknowns

$$A\vec{X} = \vec{B} \quad \text{with} \quad \vec{X} = \left(R_x, R_y, R_z, v_{\text{avg}}^2\right)^{\text{T}}, \tag{5}$$

$$\begin{pmatrix} (x_0 - x_1) & (y_0 - y_1) & (z_0 - z_1) & \left({t_0}^2 - {t_1}^2\right)/2 \\ \vdots & \vdots & \vdots & \vdots \\ \vdots & \vdots & \vdots & \vdots \\ \vdots & \vdots & \vdots & \vdots \\ (x_0 - x_n) & (y_0 - y_n) & (z_0 - z_n) & \left({t_0}^2 - {t_n}^2\right)/2 \end{pmatrix} \begin{pmatrix} R_x \\ R_y \\ R_z \\ v_{\text{avg}}^2 \end{pmatrix} = \begin{pmatrix} \left({x_0}^2 - {x_1}^2 + {y_0}^2 - {y_1}^2 + {z_0}^2 - {z_1}^2\right)/2 \\ \vdots \\ \vdots \\ \vdots \\ \left({x_0}^2 - {x_n}^2 + {y_0}^2 - {y_n}^2 + {z_0}^2 - {z_n}^2\right)/2 \end{pmatrix}.$$

Both "A" and "B" are known and can be constructed from source positions and first arrival times. Therefore, solving this linear system should give us the OBS position and the average water layer velocity. But this will not work correctly yet; the third column of the matrix "A" is $z_0 - z_i$, which, in our OBS acquisition model (Fig. 2), corresponds to the difference between depths of two sources and is generally equal to zero (as in practice all sources are often at the same depth). The same applies for $z_0 - z_i$ in vector "B". This not only means that matrix "A" is now noninvertible, but also that if a singular value decomposition (SVD) solver was used (which would decompose the matrix "A" as shown in Eq. (10) instead of directly inverting it), one would still be unable to solve for the OBS depth R_z. In fact, the OBS depth could be deduced only if the sources were placed at different depths relative one to the other. This is often referred to in the target localization field as a sensor placement problem, which adds a second layer of "complexity" that needs to be resolved.

The method proposed in this paper eliminates the sensor placement problem by employing a two-step approach: the first step is to compute R_x, R_y, and v_{avg}^2, and then compute R_z in the second step. The core principle of multilateration will again be used by computing this time the differences of offsets between a given source-receiver pair and all the other pairs. Figure 3 depicts a simple two-dimensional sketch of this scenario. In Fig. 3, the entity Offset_i is the lateral distance between shot location S_i and the OBS position, and is expressed as

$$\text{Offset}_i = \sqrt{d_i^2 - \Delta_z^2}, \tag{6}$$

which means

$$\text{Offset}_i^2 - \text{Offset}_1^2 = d_i^2 - d_1^2, \tag{7}$$

which translates in the case of multiple source locations, to the corresponding linear system on three unknowns

$$A\,\overrightarrow{X} = \vec{B} \quad \text{with} \quad \vec{X} = \left(R_x, R_y, v_{\text{avg}}^2\right)^{\text{T}}, \tag{8}$$

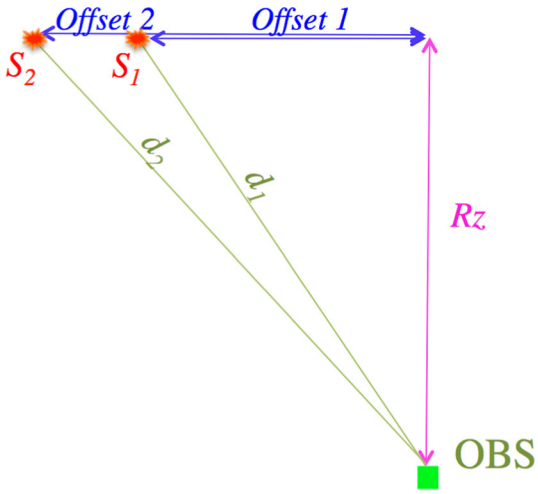

Fig. 3 Two-dimensional sketch of two shot locations

$$\begin{pmatrix} (x_0 - x_1) & (y_0 - y_1) & \left(t_0{}^2 - t_1{}^2\right)/2 \\ \vdots & \vdots & \vdots \\ \vdots & \vdots & \vdots \\ \vdots & \vdots & \vdots \\ (x_0 - x_n) & (y_0 - y_n) & \left(t_0{}^2 - t_n{}^2\right)/2 \end{pmatrix} \begin{pmatrix} R_x \\ R_y \\ v_{\text{avg}}^2 \end{pmatrix} = \begin{pmatrix} \left(x_0{}^2 - x_1{}^2 + y_0{}^2 - y_1{}^2\right)/2 \\ \vdots \\ \vdots \\ \vdots \\ \left(x_0{}^2 - x_n{}^2 + y_0{}^2 - y_n{}^2\right)/2 \end{pmatrix}.$$

Now that the OBS easting and northing is obtained, plus the average water layer velocity, the second step is to use the Pythagorean theorem and all source locations S_i. The OBS depth can then be deduced by using some statistical measure of all R_{zi}

$$R_{zi} = \sqrt{d_i^2 - \text{Offset}_i^2}. \tag{9}$$

Theoretically, using four shot locations would be enough to build a linear system of three equations and three unknowns, as in Eq. (8), and to compute R_x, R_y, and v_{avg}^2. But in the practical reality, the first arrival time values, as well as the source coordinates, always contain some uncertainties and are not as accurate as would be desired. Therefore, a large number of shots should be used to build a statistically converging system and to compensate for those errors. Moreover, one should not try directly to invert the matrix "A". Instead, a robust linear solver capable of handling

such variations in the input data has to be used to solve the linear system in Eq. (5) or Eq. (8). In this case, the solution was implemented using a solver based on SVD, which uses orthogonal matrices to reduce the matrix "A", thus minimizing the risk of magnifying inaccuracies in the input data.

SVD methods are based on the following theorem of linear algebra: any m by n matrix A with m larger or equal to n (overdetermined matrix), can be written as the product of an m by n column-orthogonal matrix U, an n by n diagonal matrix W with positive or zero elements (the singular values), and the transpose of an n by n orthogonal matrix V. The matrices U and V are each orthogonal in the sense that their columns are orthonormal as shown in Eq. (10) (Vetterling et al. 2002)

$$\begin{pmatrix} \\ A \\ \\ \end{pmatrix} = \begin{pmatrix} \\ U \\ \\ \end{pmatrix} \begin{pmatrix} w_1 & & & \\ & w_1 & & \\ & & \cdots & \\ & & & w_n \end{pmatrix} \begin{pmatrix} \\ V^T \\ \\ \end{pmatrix}. \tag{10}$$

Once the matrix "A" is decomposed, a back substitution routine is used to find the vector of unknowns "X" as shown in Eq. (11) (Vetterling et al. 2002)

$$\begin{pmatrix} \\ X \\ \\ \end{pmatrix} = \begin{pmatrix} \\ V \\ \\ \end{pmatrix} \begin{pmatrix} \\ diag(1/w_j) \\ \\ \end{pmatrix} \begin{pmatrix} \\ U^T \\ \\ \end{pmatrix} \begin{pmatrix} \\ b \\ \\ \end{pmatrix}. \tag{11}$$

To implement this inversion, a single source line (one seismic transect) cannot be used unless the transect is curved. Figure 4 shows how a single straight line (case A) cannot distinguish between a left-sided and a right-sided receiver, because, indeed, both positions are valid solutions to the same system of equations. When the source

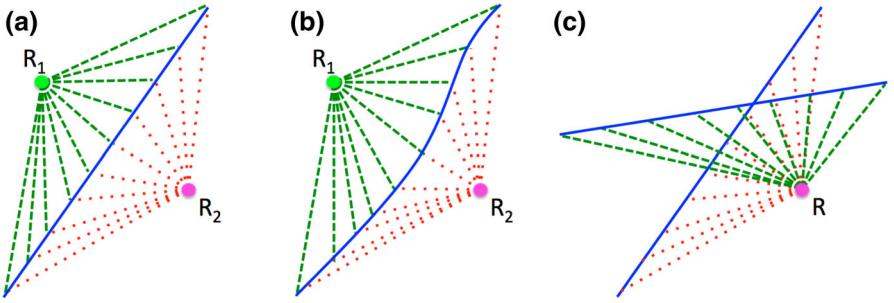

Fig. 4 Multiple scenarios of source lines, **a** a single straight source line, **b** a single curved source line, and c two crossing source lines

line is curved (case B), first arrival times are no longer symmetric and, therefore, the inversion is constrained toward the area containing the proper solution. Using two or more crossing lines (case C) ensures more constraints on the inversion process. This is the same conclusion drawn by Ao et al. (2010).

The very first test of the method is done with a synthetic model using five source lines, each with 50 shot locations, and a receiver placed between the lines at a depth of 2160 m; the water layer velocity used in this test is a constant 1500 m/s. The objective of the test is not to mimic real field conditions, but simply to validate the concept. The depth of the OBS and acquisition geometry were taken arbitrarily with the only consideration of having crossing source lines. Figure 5a shows the geometry of the shot lines, while Fig. 5b shows the corresponding first arrival of each line.

For the first test, the source depth was set to random values between 0 and 300 m, the corresponding first arrival times were used to run the inversion, as in Eq. (5). For the second test, the source depth was set to a constant depth value of 6 m, which mimics normal field conditions, the corresponding first arrival times were used to run the inversion in Eq. (8), followed by Eq. (9), to get the depth of the OBS node. Both inversions gave results with 100% accuracy because the water layer velocity used in this model is constant and the first arrivals were computed and not picked; this eliminated all sources of inaccuracy in the inversion.

4 Propagation in the Water Layer

One of the important assumptions to note is that Eq. (2) assumes that a straight ray path with a certain average sound speed can fairly approximate the propagation of seismic waves in the water layer. This is a crude approximation of reality and is only valid for near vertical propagation. At large offsets, however, the ray path is usually curved, since it is well known that sound speed in the water layer changes significantly (up to a few %) with depth.

In this paragraph, the consequences of ray propagation in a vertically heterogeneous water layer is investigated in terms of: (i) travel-time accuracy of the straight ray approximation, and (ii) maximum range of direct arrivals to be recorded before refracted energy start showing up first. The first layers of the water layer are usually strongly influenced by climatology and may exhibit strong variations of sound speed throughout the year. The dataset used in this analysis is from the Mediterranean Sea, at 7.5°E 39.5°N. Figure 6 shows a sound speed profile collected in this area in December, 2006. Rays were traced in this vertically heterogeneous model by integrating the ray equation using a simple Euler rule. The ray-tracing results are shown in Fig. 7. The simulation was run to a depth of 1500 m. Figure 7 has a large vertical exaggeration in order to clearly depict the bending of the rays caused by the heterogeneous sound speed structure. Note the maximum offset attained by the direct rays that would be recorded at the seafloor is about 8.0 km (that is to say, for this velocity structure, the first arriving energy at offsets greater than about 8.0 km will be refracted energy through the sub-seafloor strata). The travel-time at this offset limit is 5.4 s.

To evaluate the impact of a straight-ray assumption, a differential comparison of the travel-time of the rays arriving at the sea-bottom along straight lines versus bent ray

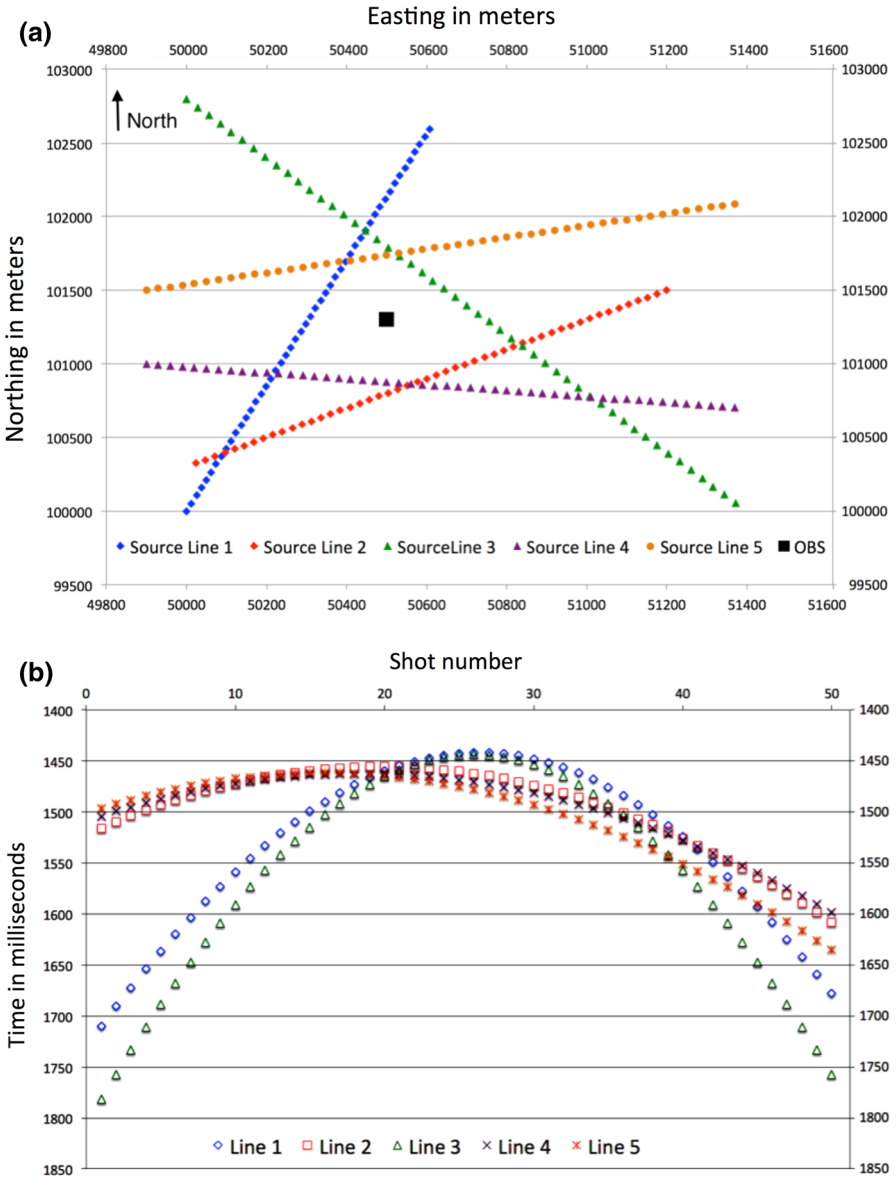

Fig. 5 Synthetic dataset composed of five source lines, each of them with 50 shot locations: **a** a map view of the acquisition geometry, and **b** first arrival times corresponding to each source line

path was performed; the results of this comparison are shown in (Fig. 8). The straight rays used in this differential comparison were computed using a constant velocity of 1500 m/s; however, the proposed method would invert for an optimized average water layer velocity making these differential errors even smaller. In this example, the differential travel time error is larger than 9 ms at 8 km offset, and only 4 ms at 5 km

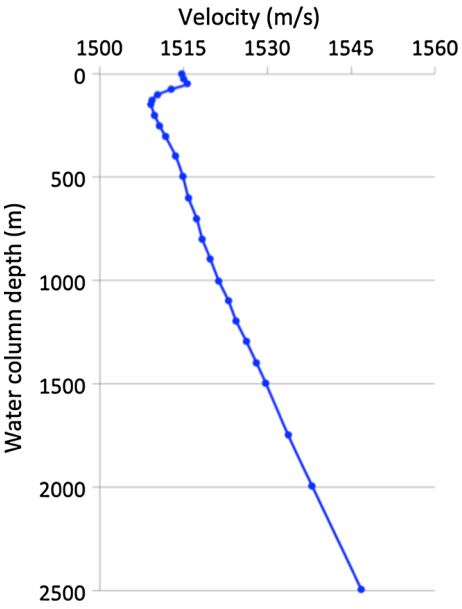

Fig. 6 Sound speed profile extracted from a climatological database for December, 2006 at a point with coordinates (7.5°E 39.5°N)

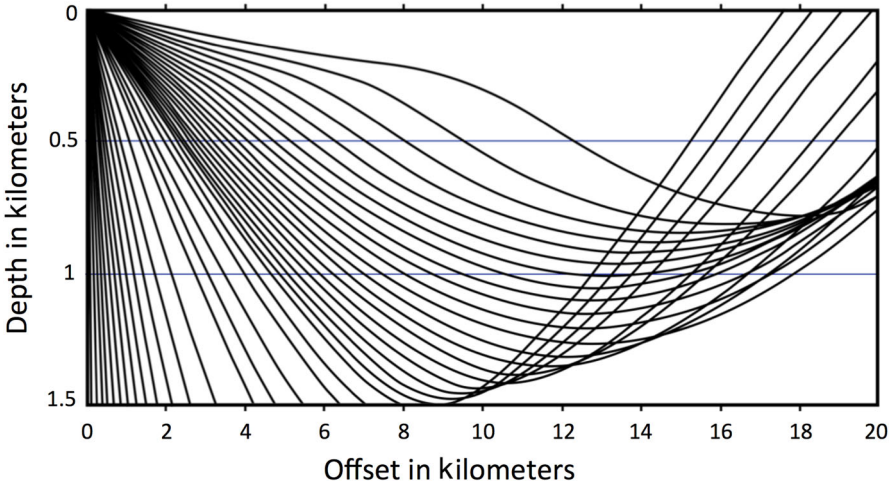

Fig. 7 Ray tracing in the vertically heterogeneous water layer velocity model of Fig. 6

offset. The effect of the bending rays will appear, for a constant velocity model, as if the average sound speed in water increases with offset (the travel-time is smaller than for a straight ray path).

There are two major conclusions from this analysis: (i) the variable sound speed in the water layer implies a critical range ($\sim$ 8 km in this example) beyond which there is no direct ray-path; (ii) at large offsets, the travel-time should be smaller than a constant velocity layer, meaning that the apparent sound speed will be larger ($\sim$ 0.2% at 8 km offset in this example).

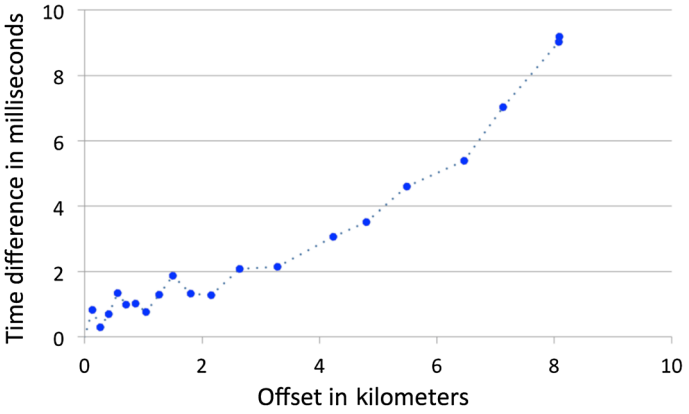

Fig. 8 Difference between the travel-times computed for a straight ray path and curved rays

Therefore, the use of first arrival picks in the near offset should be favoured, and will provide a higher accuracy positioning.

5 Application to Field Dataset: Green Canyon Dataset

The OBS location GC001 was used for this test and the first arrival times from a number of shots from multiple surrounding lines were picked (more than 3000 shot locations). Figure 9 shows the geometry of the source lines in blue, in red are the shot locations used for the inversion process, and in green is the inverted position of the OBS GC001. The maximum offset used in this test is about 2.5 km, meaning the average water layer approximation and the straight ray propagation should provide good accuracy.

The picked first arrival times, together with the known position $x/y/z$ of each source location, were used to build the matrix "A" and vector "B", as in Eq. (8). After running the inversion as shown in Eqs. (8) and (9), the travel-time of first arrivals from each source to the inverted OBS position is forward computed using the inverted average water layer velocity. A differential error is then computed between this first arrival's travel-time and the picked first arrivals (Fig. 10). The differential errors range is about $\pm$ 12 ms. The magnitudes of the differential error (absolute values) were sorted in an ascending order to further assess the accuracy of this inversion (Fig. 11). The graph in Fig. 11 shows that more then 80% of the picks (2500 picks) have an error with a magnitude of less than 5 ms. The average and median errors are 3.06 and 2.56 ms respectively. These are very satisfactory results, given that the seismic data were sampled at 5 ms; this indicates the differential errors are within the accuracy limits allowed by the picks of the first arrival times used as input data in the inversion.

In order to assess the effect of azimuthal distribution of shot locations and the total number of shots used for the inversion, a test was designed running 11 experiments with the same inversion process removing two or three arbitrarily selected source lines each time (Fig. 12). The results of these experiments were compared with the

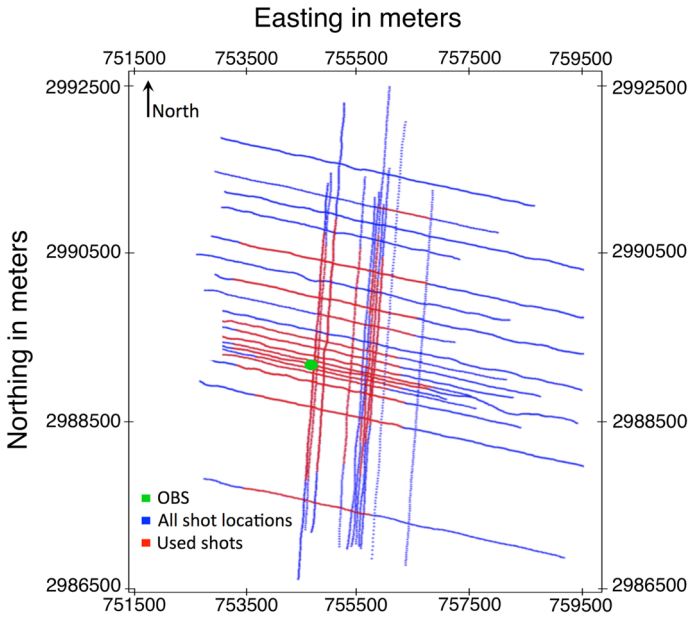

Fig. 9 A map view showing the position of the shots used for the positioning algorithm and the actual OBS position. The vertical and horizontal axes are northing/easting with UTM zone 15N

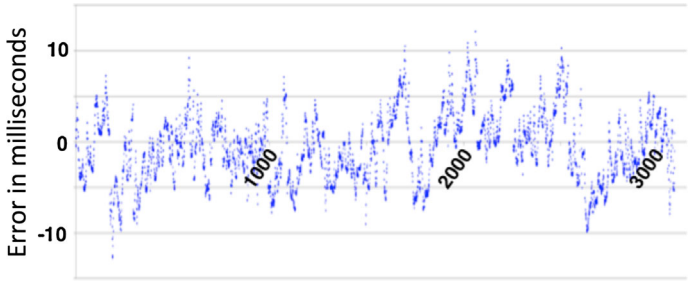

Fig. 10 Differential error of travel-time of first arrivals. Vertical axis is the error in milliseconds and the horizontal axis is the trace number

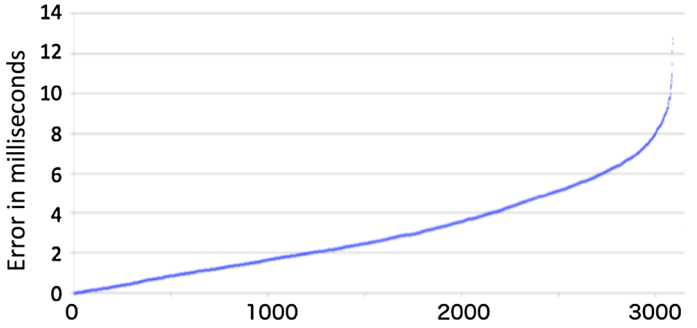

Fig. 11 Magnitude of the differential error of travel-time of first arrivals sorted in an ascending order

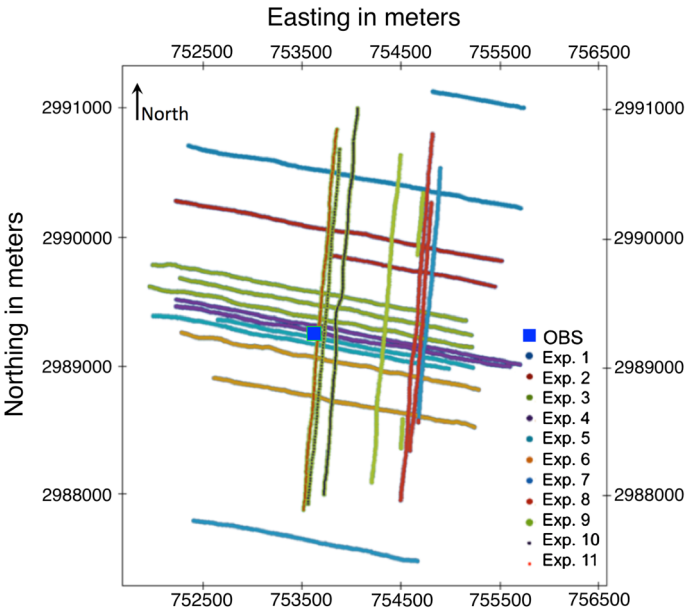

Fig. 12 Source lines used in each experiment (1–11). The blue box shows the OBS position. The vertical and horizontal axes are northing/easting with UTM zone 15N

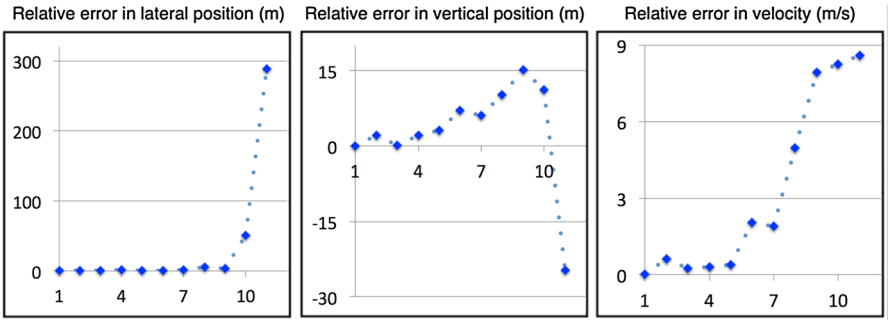

Fig. 13 Relative errors in the OBS lateral/vertical position and average water layer velocity computed with different inversion scenarios, the horizontal axis refers to the experiment number as in Fig. 12

original inversion (using all source lines) in terms of lateral drift, vertical position, and the average water layer velocity. Figure 13 shows the results of this comparison as relative errors. The azimuths of each source/receiver pair of all traces used during each experiment were also computed and are shown in Fig. 14.

Figures 13 and 14 show that experiments 1–9 have wide azimuthal coverage and they all give a very similar lateral position (within 5 m). Experiments 10 and 11 have very poor azimuthal coverage in the angle range between about $\pm$ 40° and $\pm$ 60°, respectively, and give a lateral position error of approximately 50–300 m. However, the error in vertical position follows almost a linear trend (up to 15 m) with the number of picks used, except in the last experiment where the error jumps to 36 m. Regarding the error in the average water layer velocity, three groups can be identified; the first

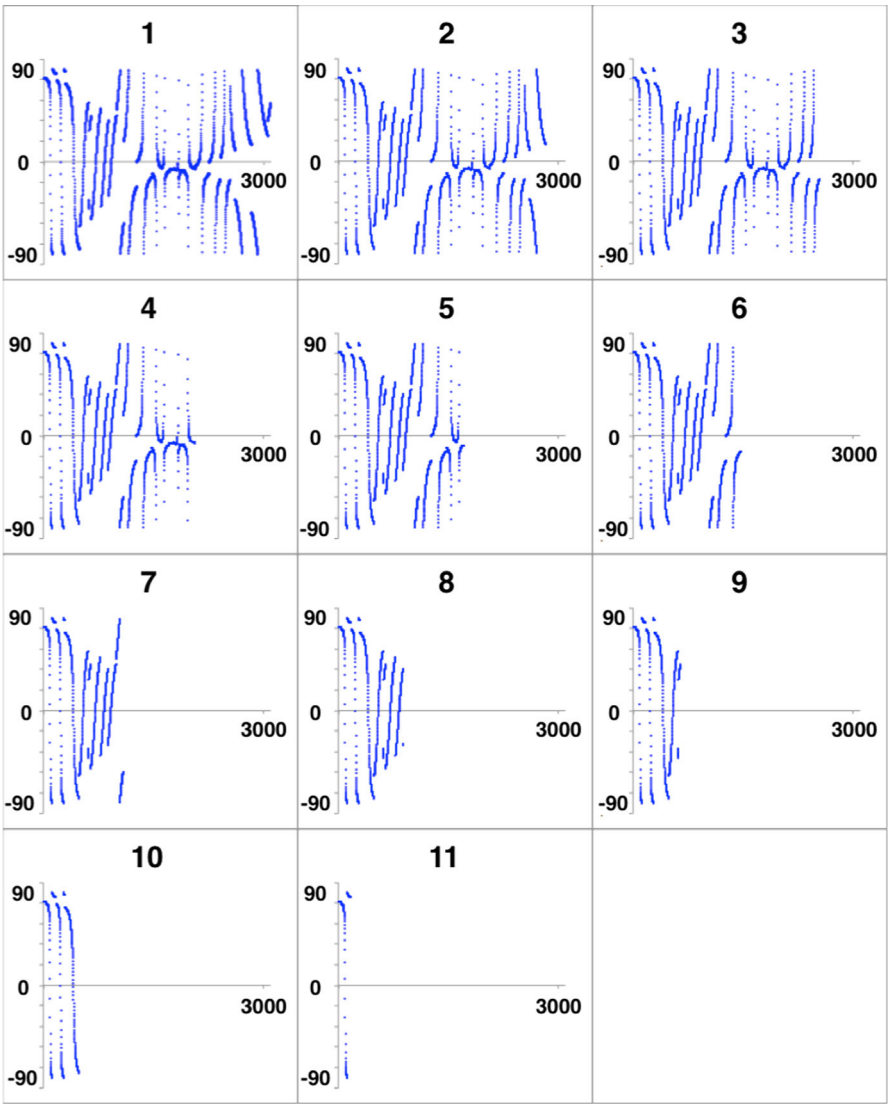

Fig. 14 Each graph shows in vertical axis the azimuthal angle of each source/receiver pair used in the inversion, in degree, and in horizontal axis the number of picks used (source locations). The number on top of each graph is the experiment number and is the same as in Fig. 12

one with an error of less then 0.5 m/s, the second increases almost linearly to up to 5 m/s error, while the last group (experiments 9, 10, and 11) reaches an error of 8 m/s.

Based on this comparison, the lateral position is affected the most by the azimuthal coverage, while the number of picks used affects equally the vertical position and the average water velocity. In general, higher azimuthal coverage and larger number of picks (within the short offsets used in this experiment) are naturally preferred, while small azimuthal coverage and small number of picks are going to result in lower

accuracy. A larger number of picks naturally increases the quality of the results, as it provides better statistics, while higher azimuthal coverage smears directional artefact caused by the heterogeneity of the water layer. For most applications in seismic data processing, 10 m accuracy in both lateral and vertical positions is very satisfactory; a scenario, at least as in experiment 9, will lead to reasonable results.

6 Conclusions

The method developed by Benazzouz et al. (2015) was further discussed in this paper and tested with an industrial-like dataset. The method efficiently rewrote the problem of OBS positioning into a linear form, removed additional complexities related to sensor placement, and delivered very satisfactory positioning results. The accuracy of the positioning is mostly influenced by the azimuthal distribution of the shot locations. While the total number of first arrival time picks impacts the accuracy, it has less weight. Using a larger number of first arrival time picks mostly compensates for inaccuracies in the first arrival time picks. The use of SVD for the linear solver gives extra robustness, as SVD is an established technique for handling inaccuracies in the input data.

Acknowledgements The authors would like to thank Parallel Geoscience Corporation for supporting this work and for granting permission to publish and discuss this paper.

References

Ao W, Zhao M-H, Qiu X-L et al (2010) The correction of shot and OBS position in the 3D seismic experiment of the SW Indian Ocean ridge. Chin J Geophys 53:1072–1081. https://doi.org/10.1002/cjg2.1577

Benazzouz O, Pinheiro L, Herold D, Afilhado A (2015) Accurate Ocean-bottom seismometers positioning using multilateration technique OBS positioning. SEG Tech Progr Expand Abstr 2015, pp 130–134. https://doi.org/10.1190/segam2015-5824940.1

Domingo-Perez F, Lazaro-Galilea JL, Wieser A et al (2016) Sensor placement determination for range-difference positioning using evolutionary multi-objective optimization. Expert Syst Appl 47:95–105. https://doi.org/10.1016/j.eswa.2015.11.008

Haines SS, Hart PE, Ruppel CD et al (2014) Cruise Report for P1-13-LA, U.S. Geological Survey Gas Hydrates Research Cruise, R/V Pelican April 18 to May 3, 2013, Deepwater Gulf of Mexico. https://doi.org/10.3133/ofr20141080

Imtiaz A, Nguyen B, Roberts M (2013) Joint inversion for ocean bottom node position and average water velocity along the shot line. In: 93rd International exposition and annual meeting SEG. Houston, pp 4880–4884. https://doi.org/10.1190/segam2013-1240.1

Mantilla Gaviria IA, Leonardi M, Balbastre-Tejedor JV, de los Reyes E (2013) On the application of singular value decomposition and Tikhonov regularization to ill-posed problems in hyperbolic passive location. Math Comput Model 57:1999–2008. https://doi.org/10.1016/j.mcm.2012.03.004

Oshida A, Kubota R, Nishiyama E et al (2008) A new method for determining OBS positions for crustal structure studies, using airgun shots and precise bathymetric data. Explor Geophys 39:15–25. https://doi.org/10.1071/EG08005

Shiobara H, Nakanishi A, Shimamura H et al (1997) Precise positioning of ocean bottom seismometer by using acoustic transponder and CTD. Mar Geophys Res 19:199–209. https://doi.org/10.1023/A:1004246012551

Vetterling WT, Teukolsky SA, Flannery BP, Press WH (2002) Numerical recipies in C the art of scientific computing. Cambridge University Press, Cambridge